## Conference paper

Liliya Yu. Kovalenko*, Vladimir A. Burmistrov, Yuliya A. Lupitskaya, Fedor A. Yaroshenko, Elena M. Filonenko and Elena A. Bulaeva

# Ion exchange of H+/Na+ in polyantimonic acid, doped with vanadium ions

**Abstract:** The influence of doping of polyantimonic acid with vanadium ions on the ion exchange $H^+/Na^+$ kinetics is determined. With the help of the X-ray analysis it is shown that doped compounds $H_2Sb_{2-x}V_xO_{6-\delta} \cdot nH_2O$, where $x = 0.14$; 0.36; 0.48 have the pyrochlore-type structure. With the increase of the amount of vanadium in a sample there is a decrease of a unit cell parameter. It is determined that there is a reduction of a unit cell frame, formed by antimonic and vanadium ions, and a size reduction of hexagonal cavities, in which protons are located. It is shown that during the ion exchange of $H^+/Na^+$ there is a change of the unit cell plane without a symmetry breaking of a crystal structure, which demonstrates solid solution formation. With the increase of the amount of vanadium in the sample there is a decrease of the ion-exchange capacity, which is connected with the decrease of the channel's section size. The ion exchange $H^+/Na^+$ kinetics has been studied with the approximation of the Boyd's model for the intergrain diffusion. Diffusion coefficients had the order $10^{-13}$ m²/s and decreased with the increase of the amount of vanadium in the sample.

**Keywords:** diffusion coefficient; ion exchange; isovalent doping; polyantimonic acid; solid electrolytes; SSC-2018.

## Introduction

The characteristic feature of inorganic cation exchangers is the presence of the plane, formed by tetrahedral or octahedral groups of oxide, phosphate and cyanide groups [1, 2]. Such an open plane cavity structure has a negative charge, which is compensated by counter ions (protons, metal, ammonium, alkyl ammonium cations and other ions). Due to the fact that at the rate-controlling step of the ion exchange in the solid state the cation passes through the shared edge of two coordination polyhedrons within the crystal, the channel section's size, formed by the anionic atoms, is the essential condition [3, 4].

One of the perspective cation exchangers for the separation of alkali ions, which are difficult to be separated by means of other methods, is the polyantimonic acid (PAA) $H_2Sb_2O_6 \cdot nH_2O$, $2 < n < 5$, crystallized within the pyrochlore-type structure (sp. gr. *Fd3m*). In the distribution of polyantimonic acid atoms over crystallographic positions within the pyrochlore-type structure, 8*b* positions are left unoccupied. As a result, a skeletal plane of the defect structure, consisting of [SbO₃] – octahedrons, connected by apexes, is formed; it has channels with hexagonal cavities, in which protons are located. Due to the large size of the channels, their symmetric location, cations of monovalent and bivalent ions can be placed inside them, depending on

*Corresponding author: Liliya Yu. Kovalenko, Chelyabinsk State University, 129, Br. Kashirinyh St., Chelyabinsk 454001, Russia, e-mail: lkovalenko90@mail.ru. https://orcid.org/0000-0002-9187-6934
**Vladimir A. Burmistrov, Yuliya A. Lupitskaya, Fedor A. Yaroshenko, Elena M. Filonenko and Elena A. Bulaeva:** Chelyabinsk State University, 129, Br. Kashirinyh St., Chelyabinsk 454001, Russia

the radii of the last ones, and the presence of a hydration shell [5, 6]. One of the methods, which increases the sorption selectivity, is the composition change of PAA plane by means of iso- and heterovalent doping. For instance, the implementation of the small amount of a isovalent ion such as vanadium (+5) that has a larger size in comparison with the antimonic ions (+5), may lead to the reduction of the channel's size.

In this regard this work is aimed at defining the ion-exchange capacity of PAA, doped with vanadium ions in reference to $Na^+$ ions, studying the ion exchange kinetics, determining the rate-controlling step in the process of exchange, calculating of interdiffusion coefficients.

## Experimental

Samples preparation has been made with the help of the co-precipitation method by adding the solution of sodium vanadate dropwise of preset concentration to the antimony trichloride solution, preoxidized by nitric acid, according to the methodology, described in [7, 8]. The resulting residue has been separated from the mother liquor, flushed with distilled water until the negative reaction of the filtrate to the chloride ions has been observed, and air-dried. After that the sample has been ground in the agate mortar, has been tempered at a temperature of 450 K for the further crystallization of the product and has been allowed to stand for a long time at room temperature in normal conditions ($T = 298$ K, air humidity ~70 %).

The elemental analysis of the synthesized compounds has been conducted with the help of ED-XRF Oxford INCA X-max 80, set on the scanning electron microscope JeoL JSM 7001F. The elemental composition of the samples has been determined with the consideration of energy dispersive spectrometry. The local energy dispersive microanalysis has been conducted in different parts of samples.

NEXAFS measurements in the area of the vanadium ions energy absorption have been made by means of X-ray photoelectron spectroscopy method involving the K-Alpha System by Thermo Fisher Scientific. During this process the energy resolution was $0.1 \div 0.2$ eV, the accuracy of element binding in energy was at least 0.1 eV. Stable oxides of 3$d$-elements have been used as standard, the comparison of obtained spectra of simple and composite oxides with the spectra from the literature sources has been carried out.

The EPR spectra have been recorded with the help of RE-1306 radiospectrometer at room temperature, in which the resonance condition has been reached by changing of magnetic intensity B at constant frequency. The sample MgO:$Mn^{2+}$ with the known quantity of paramagnetic centres (PMC) has been used as standard. The sample mass has been measured with the help of VLR-20 analytical balances.

Structural researches of phases, gained as a result of thermolysis, have been carried out on the X-ray diffractometer Rigaki ultima IV (filtered CuK$\alpha$-radiation) within the range of diffraction angles $10 < 2\theta < 70°$. The laws of maximum extinction have been analyzed as well as their intensity variation and interplanar spacing, which have been compared with literature data. The X-ray researches, which have been carried out with the help of the Rietveld method and the programme PowderCell 2.4, have shown the location of ions according to the regular point system of the pyrochlore-type structure sp. gr. *Fd3m* as well as the unit cell parameter, distance between the atoms. The visualization of crystallized structures in 3D-format has been made with the help of Vesta 32 programme.

Infrared absorption spectra of samples, pressed into a KBr tablet, have made registrations, regarding air on X-ray Fourier spectrometer Nicolet 380 in the frequency range from 500 to 4000 $cm^{-1}$.

The obtained samples have been ground in the agate mortar and then sieved through screens with 0.100 and 0.125 mm cells. PAA fraction has been obtained with the particles (0.112 mm in diameter).

The ion exchange of $H^+$/$Na^+$ has been conducted in NaOH solution. For that purpose the sample weight $0.5000 \pm 0.0005$ g has been placed into 100 $cm^3$ of distilled water, to which the solution of sodium hydroxide of preset concentration (0.5 M) has been poured by equal portions (0.5 ml) and mixed with at the rate of 190 rpm. The measurements of the pH suspension have been made with the help of pH-meter Multitest IPL-311, which helps to fix measurable quantities in the course of time. It is considered that a complete substitution of protons for sodium ions occurs at pH equilibrium values.

# Results and discussion

Polyantimonic acid doping with vanadium ions within the pyrochlore-type structure has a concentration limitation: substitutional solid solution $H_2Sb_{2-x}V_xO_6 \cdot nH_2O$ is formed when $0 < x < 0.48$. That is why the samples, containing 7 ($x = 0.14$), 18 ($x = 0.36$), 24 ($x = 0.48$) at. % of vanadium, according to the elemental analysis data, have been chosen as subjects of the present research.

NEXAFS-spectra of subtle texture of approximate edge of X-ray absorption of doped compounds have allowed to define the vanadium ions' valent state. The base peak position corresponds with the binding energy of 2p-electrons of ions $V^{+5}$: $E(V\ 2p) = 517.4$ eV (Fig. 1). The peak is not registered when $E(V\ 2p) = 515.7$ eV, specific for vanadium atoms in $V_2O_3$ (Fig. 1).

On the EPR samples spectra there has not been any signal, which proves that there are no valency electrons in antimony and vanadium ions. Thus, in doped compounds antimony and vanadium ions are primarily in a state of $Sb^{+5}$ and $V^{+5}$.

There is an identical set of diffraction maxima in the X-ray diffraction patterns. The law of extinction analysis (*hkl*) demonstrates that the synthesized compounds have the pyrochlore-type structure. Rietveld X-ray analysis of the compounds' structure (Fig. 2) has allowed to define the distance between ions B−O and the size of the channels' section (distance O−O).

High correlation between theoretical and practical diagrams indicates the correct choice of the model of atom arrangement in crystallographic positions of the pyrochlore-type structure (Table 1), according to which ions $Sb^{+5}$ and $V^{+5}$ are statistically placed at 16c positions of the structure and with anions of oxygen and hydroxyl groups, holding 48f-positions, form oxygen-antimony octahedrons. Oxonium ions and water molecules statistically fill 16d positions and are located in hexagonal channels. It appears that with the formation of a solid substitutional solution on the basis of polyantimonic acid there is a substitution of antimony ions with vanadium ions in the center of octahedrons, at the same time structural parameters are being changed [9–11].

During the process of polyantimonic acid doping with vanadium ions there is a reduction of the unit cell plane, formed by antimony and vanadium ions, which is proved by the reduction of the unit cell parameter and distance $d$(B−O) (Table 1). The distance reduction between oxygen atoms, located in the apexes of hexagon diagonal ($d$(O−O)) is observed. Therefore, the size of hexagonal cavities, in which protons are located, is reduced (Fig. 3).

Broad complex absorption band in the area between 3700 and 3000 cm⁻¹ is typical for stretching vibrations of water molecules and hydronium ions (Fig. 4). The peak of stretching vibrations of νOH ions lies in
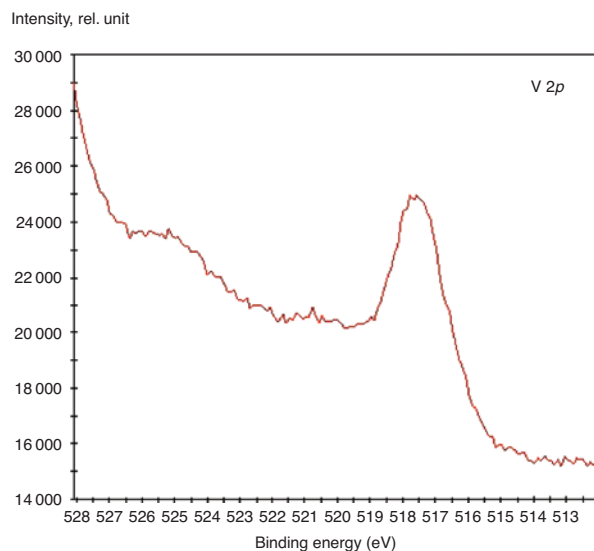


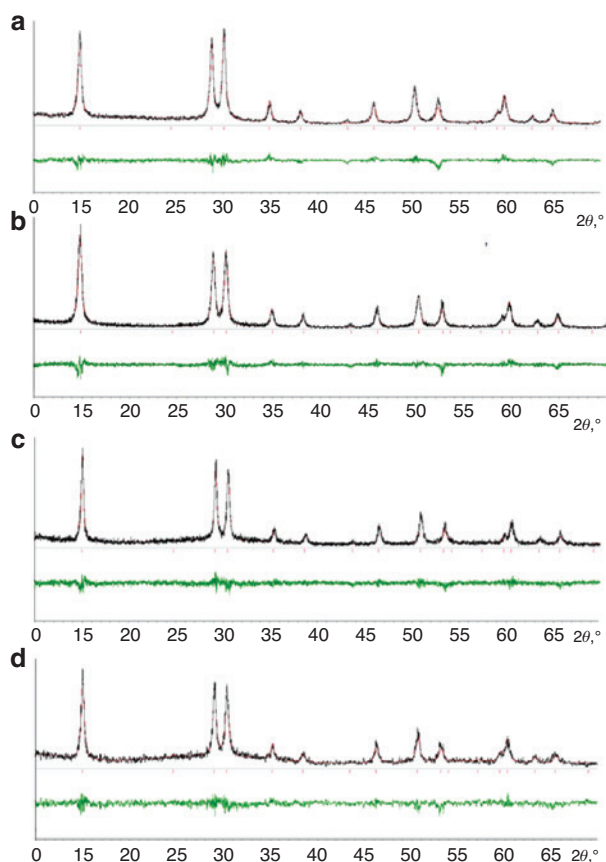**Fig. 1:** NEXAFS spectrum of the $H_2Sb_{1.86}V_{0.14}O_6 \cdot nH_2O$.

**Fig. 2:** Theoretical (red), experimental (black), difference (green) X-ray diagrams of samples' compounds $H_2Sb_{2-x}V_xO_6 \cdot nH_2O$, where $x = 0$ (a), 0.14 (b), 0.36 (c), 0.48 (d).

**Table 1:** Parameters of compounds' structure, where a – unit cell parameter, $d$(B–O) – distance B–O, B=V, Sb, $d$(O–O) – distance O–O (the rel. error has been $\varepsilon < 0.01\%$).

| Composition | $a$, Å | $d$(B–O), Å | $d$(O–O), Å |
|---|---|---|---|
| $H_2Sb_2O_6 \cdot nH_2O$ | 10.35(6) | 1.849 | 5.926 |
| $H_2Sb_{1.86}V_{0.14}O_6 \cdot nH_2O$ | 10.34(3) | 1.847 | 5.919 |
| $H_2Sb_{1.64}V_{0.36}O_6 \cdot nH_2O$ | 10.31(2) | 1.841 | 5.901 |
| $H_2Sb_{1.52}V_{0.48}O_6 \cdot nH_2O$ | 10.30(6) | 1.840 | 5.898 |

the area at 3420 cm⁻¹, which is connected with the formation of weak hydrogen bondings by OH⁻ ions. In the area of deformation vibrations δOH on the infrared spectrum there can be distinguished 4 absorption bands – broad with the maximum at 1700 cm⁻¹, narrow, strong at 1630 cm⁻¹, 1410 cm⁻¹ and 1260 cm⁻¹. The band at 1700 cm⁻¹ corresponds to deformation vibrations of hydronium ions δH₃O⁺, at 1630 cm⁻¹ there can be observed a stronger band, which is characterized by deformation vibrations of absorbed water molecules, at 1410 cm⁻¹ and 1260 cm⁻¹ – plane deformation vibrations δOH⁻. The presence of the complex band with the maximum at 1050 cm⁻¹ is characterized by the presence of δOH⁻ group deformation vibrations, located on the surface. Absorption bands at 770 cm⁻¹ и 450 cm⁻¹ correspond to stretching vibrations of the bonding νSb−O.

For doped forms a small movement of valence vibration frequencies νSb−O can be observed, the appearance of additional absorption bands is not registered, corresponding to V−O bindings [12]. The absence of
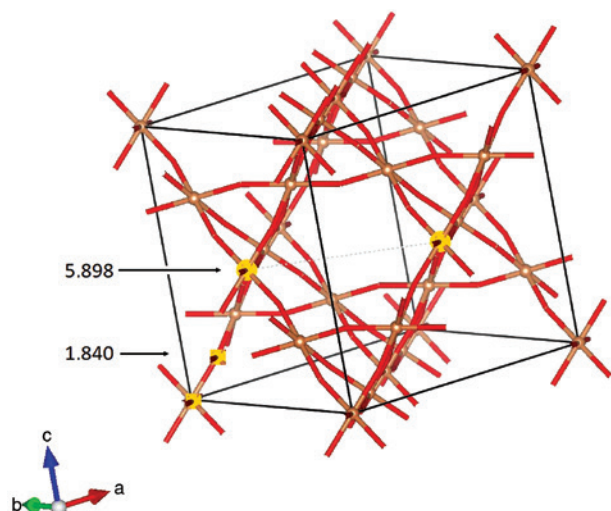
**Fig. 3:** Elementary cell of polyantimonic acid, doped with vanadium ions: $H_2Sb_{1.52}V_{0.48}O_6 \cdot nH_2O$.

these bands proves the equal distribution of vanadium ions in PAA structure and the similarity of the finger-print region of V–O and Sb–O ions (Fig. 4).

On the curve of the ion exchange H⁺/Na⁺ of PAA suspension doped with sodium hydroxide, there are regions, where the suspension pH is practically unchanged, and then increases rapidly. The process of ion exchange comes to an end, when the slope of the ion exchange curve coincides with the slope of the blank test curve (Fig. 5).

The data obtained have allowed us to construct exchange isotherms (Fig. 6), and define the quantity of the sorbing agent per unit weight of compounds in the balanced state $Q_e$ (Table 2).

The ion exchange isotherms have the form of sorption curves of microporous samples with relatively small amount of the outer surface. With the increase of vanadium quantity in the sample there is a reduction of the ion exchange capacity (Table 2), which is, probably, connected with the channel's section size (Table 1).

In the X-ray diffractograms of the samples after the ion exchange (Na⁺ – forms), there is a set of diffraction peaks (Fig. 7), which is satisfactorily identified within the framework of the cubic crystal system, and the analysis of the law of reflection extinction *(h, k, l)* proves that Na-forms of PAA have the pyrochlore-type structure, space group of symmetry *Fd3m*.

With the increase of Na⁺ ions amount in the pyrochlore phase there is a redistribution of relative intensities between different groups of reflections. For instance, relative reflection intensities with uneven indices $(h, k, l = 2n + 1)$ monotonously reduce with the increase of the ion exchange degree (Fig. 7). Reflection intensities with uneven indices for the studied samples alter considerably. Such intensity alterations may be determined by the atomic scattering factor of X-rays and filling 16*d* positions within crystallized pyrochlore-type structure with vanadium ions. At the same time in caustic solutions low intensity reflections are observed, which belong to $Na_3VO_4$ phase [13].

With regard to X-ray data about cation-exchange resin symmetry conservation during the ion exchange, redistribution of intensities clearly proves that with the increase of metal ions' amount in the solid phase the structural amplitude of the pyrochlore phase changes, and, therefore, the unit cell basis changes.

From this perspective the ion exchange is carried out by means of mutual diffusion of metal ions inside the crystal structure of the samples and hydrogen ions – out of it. This leads to the formation of substitution solid solutions and unit cell basis change without breaking the local electrical neutrality and symmetry of the crystal structure.

At the initial stage of adding the sodium hydroxide solution there is a rapid increase of suspension's pH, determined by the increase of alkali concentration (Fig. 8). In the course of time pH is reduced, and it achieves equilibrium values.
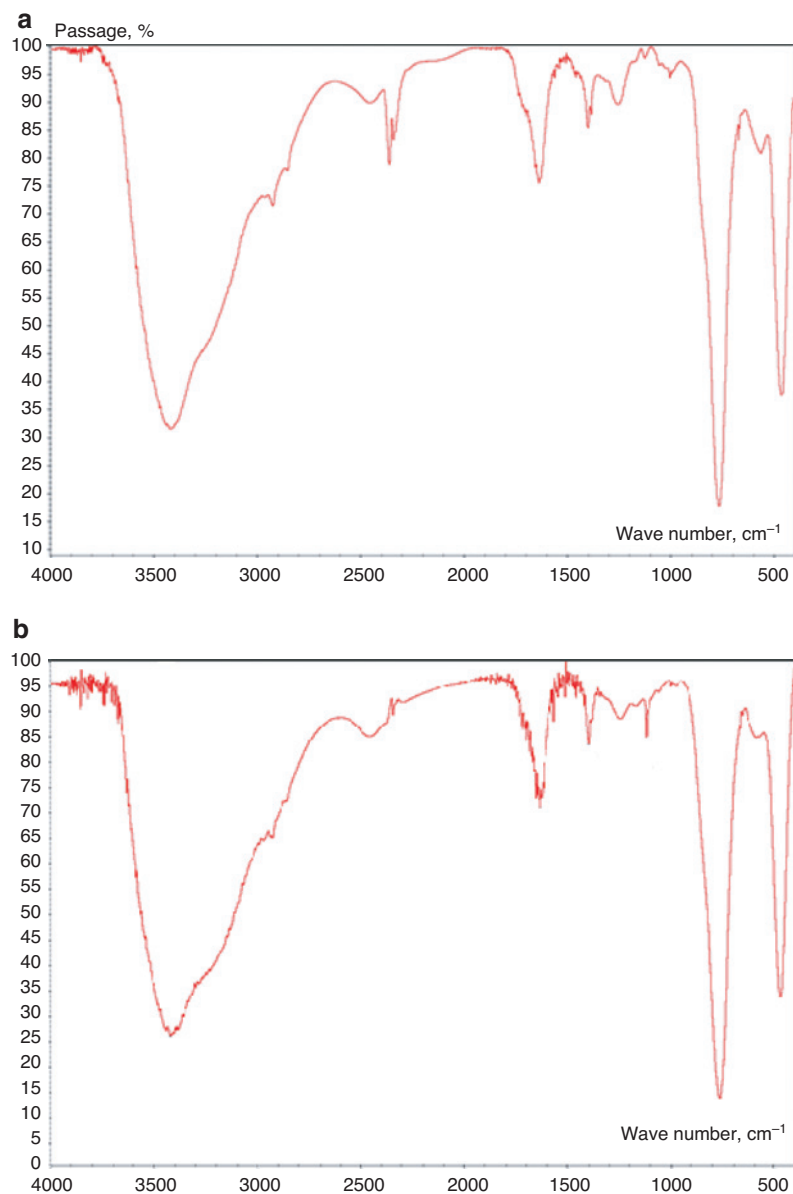
**Fig. 4:** Infrared spectrum: (a) H$_2$Sb$_2$O$_6 \cdot n$H$_2$O; (b) H$_2$Sb$_{1.52}$V$_{0.48}$O$_6 \cdot n$H$_2$O.
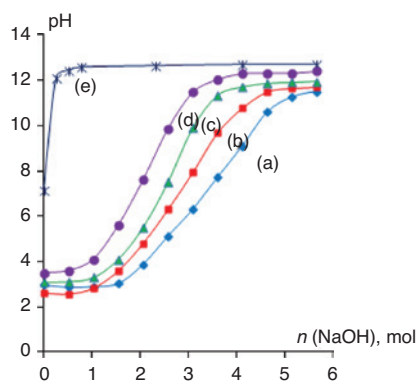


**Fig. 5:** Curves of the ion exchange H$^+$/Na$^+$ of samples' compounds H$_2$Sb$_{2-x}$V$_x$O$_6 \cdot n$H$_2$O, where $x = 0$ (a), 0.14 (b), 0.36 (c), 0.48 (d), blank test (e).
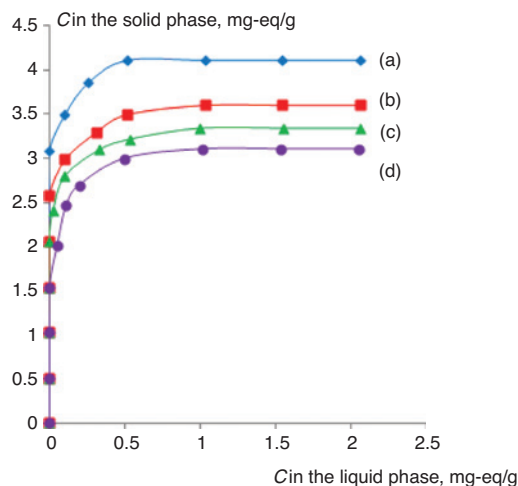
**Fig. 6:** Isotherms of the ion exchange H⁺/Na⁺ of samples' compounds $H_2Sb_{2-x}V_xO_6 \cdot nH_2O$, where $x=0$ (a), 0.14 (b), 0.36 (c), 0.48 (d).

**Table 2:** Figures of the ion exchange capacity and diffusion coefficients of H⁺/Na⁺ samples.

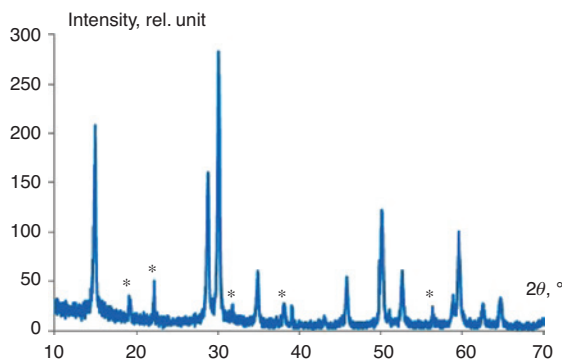| Nº of the sample | Sample composition | $Q_e$, mg-eq/g | $D \cdot 10^{13}$, m²/s |
|---|---|---|---|
| 1 | $H_2Sb_2O_6 \cdot nH_2O$ | 4.1 | 7.3 |
| 2 | $H_2Sb_{1.86}V_{0.14}O_6 \cdot nH_2O$ | 3.6 | 5.1 |
| 3 | $H_2Sb_{1.64}V_{0.36}O_6 \cdot nH_2O$ | 3.3 | 2.9 |
| 4 | $H_2Sb_{1.52}V_{0.48}O_6 \cdot nH_2O$ | 3.1 | 2.2 |



**Fig. 7:** X-ray diagram of Na-form sample $H_2Sb_{1.52}V_{0.48}O_6 \cdot nH_2O$.

The ion exchange is carried out at the particular time interval, which proves the presence of diffusion processes of proton substitution with sodium ions.

In order to define the influence of the outer mass transport on the kinetics of the ion H⁺/Na⁺ exchange in doped compounds the graphs $-\ln(1-F) = f(t)$ have been constructed. At the initial moment of the exchange time (at small values of $F < 0.2$), for all the studied ions experimental points can easily fit the linear dependence, which proves that at this substitution interval the great impact is being made by the outer mass transport (Fig. 9). The deviation of this dependence from linearity when $F > 0.3$ proves the realization of intergrain diffusion mechanism. In this case kinetic curves are described by the Boyd equation [14, 15].

In the Fig. 10 there are dependency graphs of the degree of substitution $F$ from the time t for H⁺/Na⁺, in which there can be distinguished 2 areas. The direct dependence of the process termination degree on the
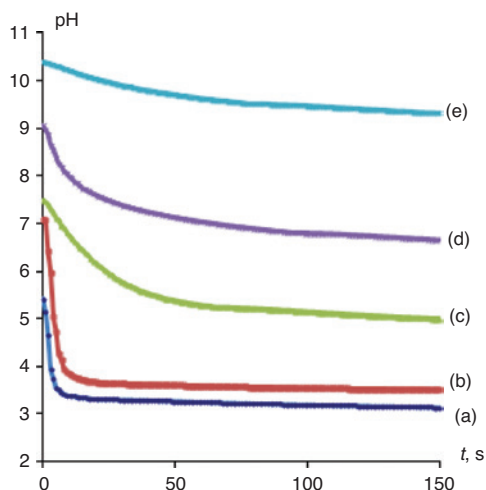
**Fig. 8:** pH relaxation after alkali pouring to $H_2Sb_{1.52}V_{0.48}O_6 \cdot nH_2O$. Protons' degree substitution: (a) 15 %; (b) 30 %; (c) 45 %; (d) 60 %; (e) 75 %.
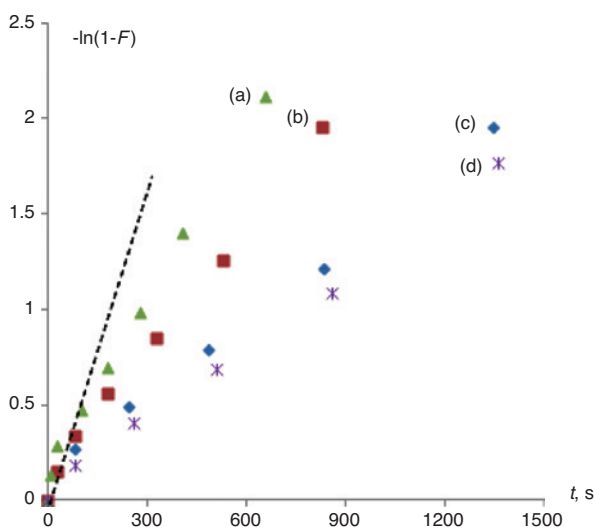


**Fig. 9:** Dependence of $-\ln(1-F)$ on the ion exchange time ($F < 0.2$, linear approximation) of samples' compounds $H_2Sb_{2-x}V_xO_6 \cdot nH_2O$, where $x = 0$ (a), 0.14 (b), 0.36 (c), 0.48 (d).

time when $0 < F < 0.3$ reflects the ions' diffusion in the solid body through a small product's layer. The change of the slope of line (when $F > 0.3$) indicates a decrease in velocity because of the ion exchange behavior being impeded due to the thickness of the product layer.

According to the experimental data, kinetic dependencies of the substitution degree, constructed in coordinates $Bt = f(t)$ represent straight lines (Fig. 11) with a different angle of slope, which prove the intergrain diffusion in the samples. Diffusion coefficients (Table 2), calculated with regard to the data, are reduced with the increase of the vanadium amount in the sample.

It appears that the ion exchange process occurs in accordance with the following mechanism: at the first stage – ions' sorption on the crystal's surface, the substitution of $H_3O^+$ for sodium ions, at the second stage – alkali ions' transportation along the channels of crystal lattice inside the grain and their statistical filling of 16d positions. Protons and $H_3O^+$ ions go into solution by means of reverse transportation and enter into a reaction with $OH^-$ – groups, which does not lead to the significant change of pH. It is possible that the limiting stage of the ion process is the diffusive mobility of sodium ions.
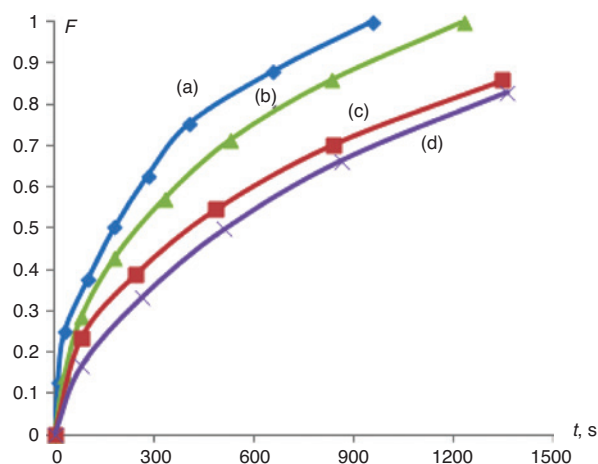
**Fig. 10:** Dependence the completion degree of substitution *F* on the ion exchange time of samples' compounds $H_2Sb_{2-x}V_xO_6 \cdot nH_2O$, where $x = 0$ (a), 0.14 (b), 0.36 (c), 0.48 (d).
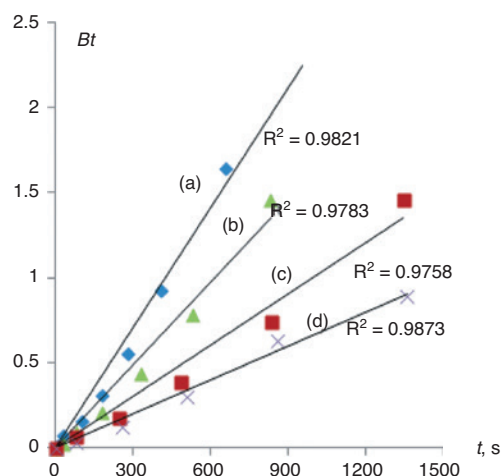


**Fig. 11:** Dependence of kinetic coefficient *Bt* on the ion exchange time of samples' compounds $H_2Sb_{2-x}V_xO_6 \cdot nH_2O$, where $x = 0$ (a), 0.14 (b), 0.36 (c), 0.48 (d).

## Conclusions

1.  The samples of polyantimonic acid, doped with isovalent vanadium ions, have been obtained with the help of a co-precipitation method. X-ray parameters of samples have been defined as well as interplanar distances, distances between atoms within the pyrochlore-type structure (according to the Rietveld method). When doping polyantimonic acid with vanadium ions there is a reduction of the unit cell plane and a reduction of channels' radius with hexagonal cavities, in which protons are located.
2.  It is shown that during the ion exchange there is a change in structural parameters, which proves the formation of solid solutions. The kinetics of the ion exchange H⁺/Na⁺ is described with the help of the Boyd model for intergrain diffusion, even though the diffusion coefficients reduce with the increase of the vanadium amount in the sample.

# References

[1] C. B. Amphlett. *Inorganic Ion Exchangers*, Elsevier, Amsterdam (1964).

[2] P. Feng, X. Bu, G. D. Stucky. *Nature* **388**, 735 (1997).

[3] A. B. Yaroslavtsev. *Russ. Chem. Rev.* **66**, 656 (1997).

[4] I. A. Stenina, A. B. Yaroslavtsev. *Inorg. Mater.* **53**, 253 (2017).

[5] A. V. Egorysheva, O. G. Ellert, O. M. Gaitko, M. N. Brekhovskikh, I. A. Zhidkova, Y. V. Maksimov. *Inorg. Mater.* **53**, 962 (2017).

[6] E. Gonzalez, R. Llavona, J. R. Garcia, J. Rodriguez. *J. Chem. Soc. Dalton Trans.* **5**, 829 (1989).

[7] F. A. Belinskaya, E. A. Militsina. *Russ. Chem. Rev.* **49**, 933 (1980).

[8] M. Abe, K. Sudoh. *J. Inorg. Nucl. Chem.* **42**, 1051 (1980).

[9] J. Chen, Z. Chen, X. Zhang, X. Li, L. Yu, D. Li. *Appl. Catal. B* **210**, 379 (2018).

[10] Y. A. Lupitskaya, D. A. Kalganov, M. V. Klyueva. *Inorg. Mater.* **54**, 240 (2018).

[11] D. Klestchov, V. Burmistrov, A. Sheinkman, R. Pletnev. *J. Solid State Chem.* **94**, 220 (1991).

[12] K. Nakamoto. *Infrared and Raman Spectra of Inorganic and Coordination Compounds: Part A: Theory and Applications in Inorganic Chemistry*, Sixth ed., John Wiley & Sons, New York (2009).

[13] M. G. Barker, A. J. Hooper. *J. Chem. Soc. Dalton.* **15**, 1513 (1973).

[14] M. Outokesh, A. Naderi, A. R. Khanchi, J. Karimi Sabet. *Ind. Eng. Chem. Res.* **53**, 305 (2013).

[15] H. Costa, R. M. C. Vegas, M. Rosa, M. Campinas. *Adsorption* **20**, 737 (2014).